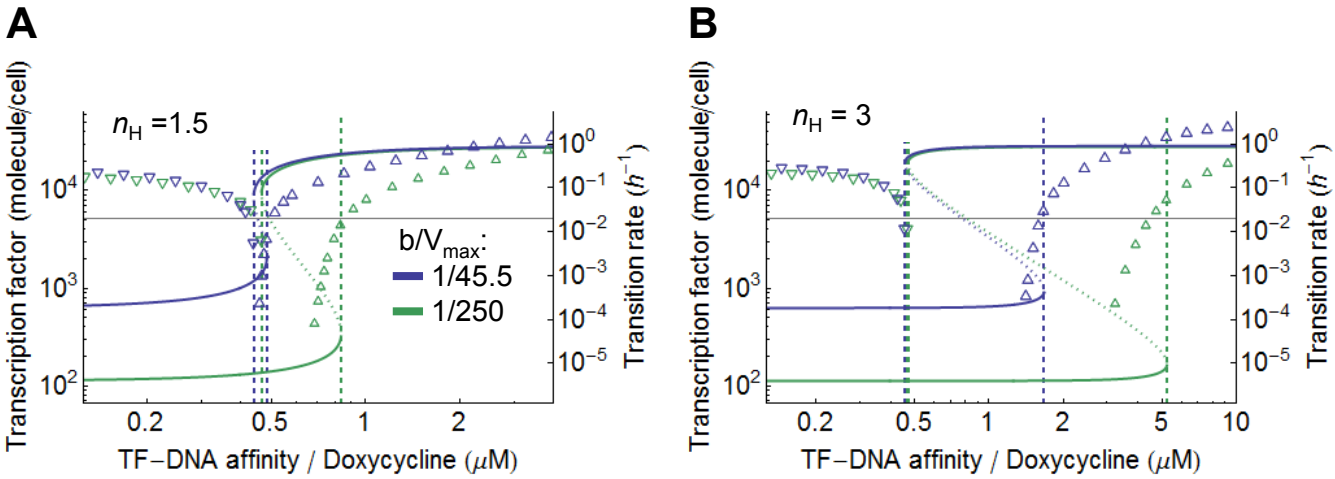

C

Vmax/b	Hill coef. (n_H)	Left boundary, Doxycycline (μM) exact	estimated	% error	Right boundary, Doxycycline (μM) exact	estimated	% error
250	1.5	0.4667	0.4492	-3.8	0.8357	0.8524	2.0
45.5	1.5	0.4406	0.4282	-2.8	0.4842	0.5038	4.0
250	2	0.4954	0.4629	-6.6	1.9767	1.8851	-4.6
45.5	2	0.4775	0.4794	0.4	0.8432	0.8434	0.0
250	3	0.4699	0.4628	-1.5	5.2364	4.4320	-15.4
45.5	3	0.4571	0.4498	-1.6	1.6674	1.6207	-2.8

Fig. S1 Accuracy of the approximation of the bistable boundaries by a threshold of transition rate at 0.02 (h^{-1}) in feedback loops with weakly and strongly cooperative binding of the TF. (A,B) The same parameters were used as in Fig. 1A,C, except for the Hill coefficient n_H = 1.5 in (A) and 3 in (B). (C) The exact bifurcation points are compared with the estimated ones at threshold of transition rate 0.02 (h^{-1}). The relative errors are calculated for each value of basal expression.

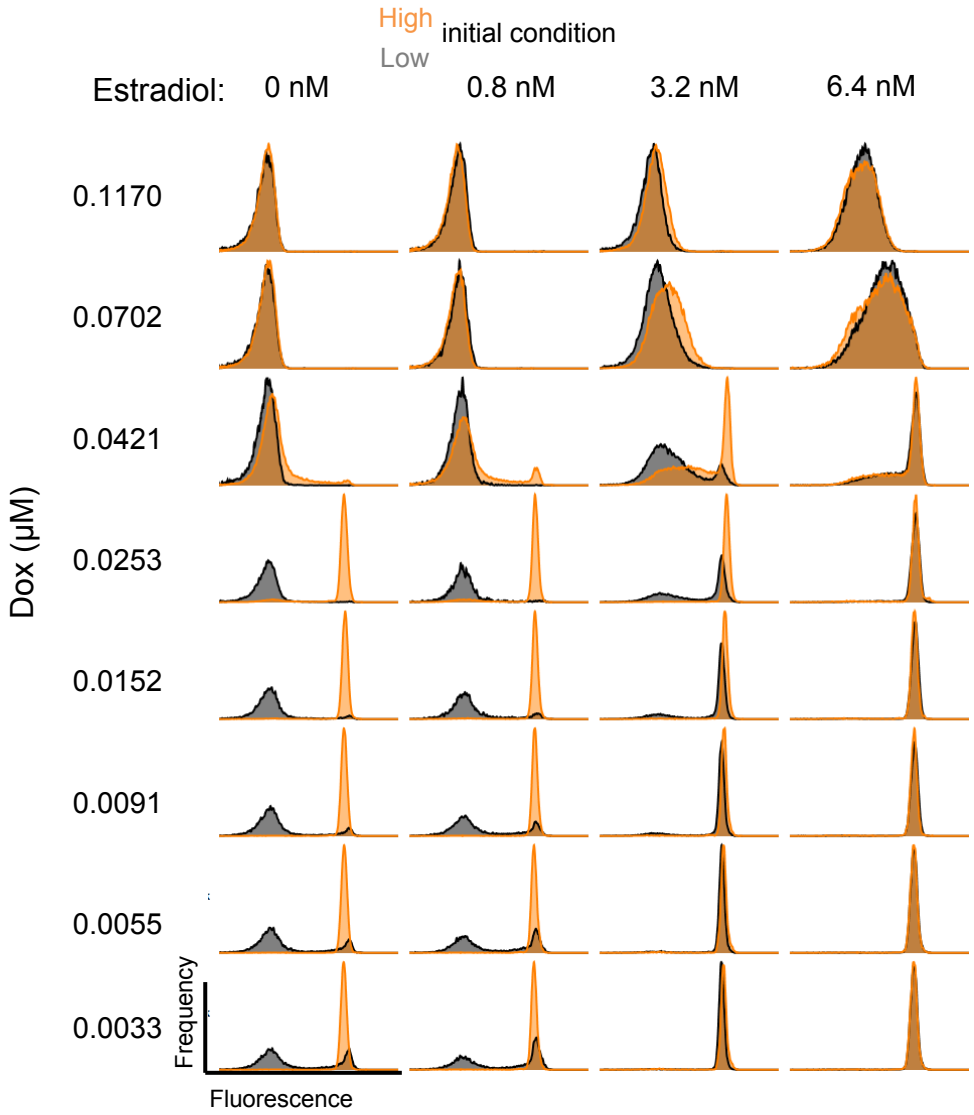

Fig. S2 Histograms of fluorescence distributions of the $P_{[tetO]1}$-tTA feedback loop as doxcycycline and estradiol is varied The low and high initial conditions were set by incubating the cells in the absence or presence of galactose (at 0.5%). Measurements were performed after transferring the cells from the above initial conditions into the media with the indicated doxycycline concentration and estradiol and were grown for an additional 24h. The tTA activity in the feedback loops in the cells was reported with GFP. This figure is related to Fig. 3A.

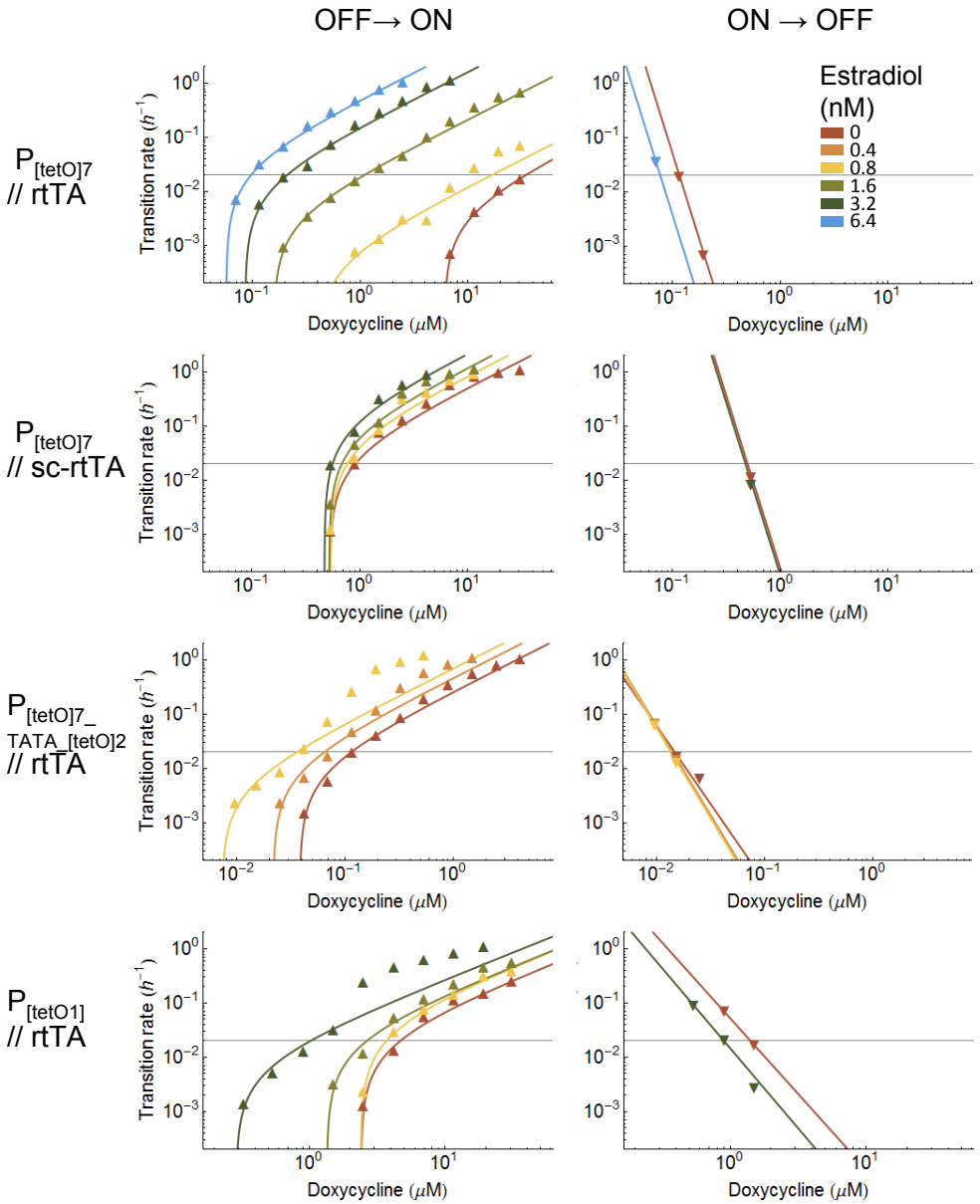

Fig. S3 Measured transition rates between the two expression states in feedback circuits. The transition rates from OFF to ON (left panels) and from ON to OFF expression states (right panels) for 4 different feedback loops were plotted as function of doxycycline concentration. The feedback expression range was adjusted by the estradiol concentration which controls the basal expression (see methods). At each feedback expression range, the OFF-to-ON and ON-to-OFF transition rates were fitted as function of doxycycline concentration by a linear regression and by a power regression, respectively. The threshold used in Fig. 3B and 5A (gray horizontal lines) was set at 0.02 h^{-1}.

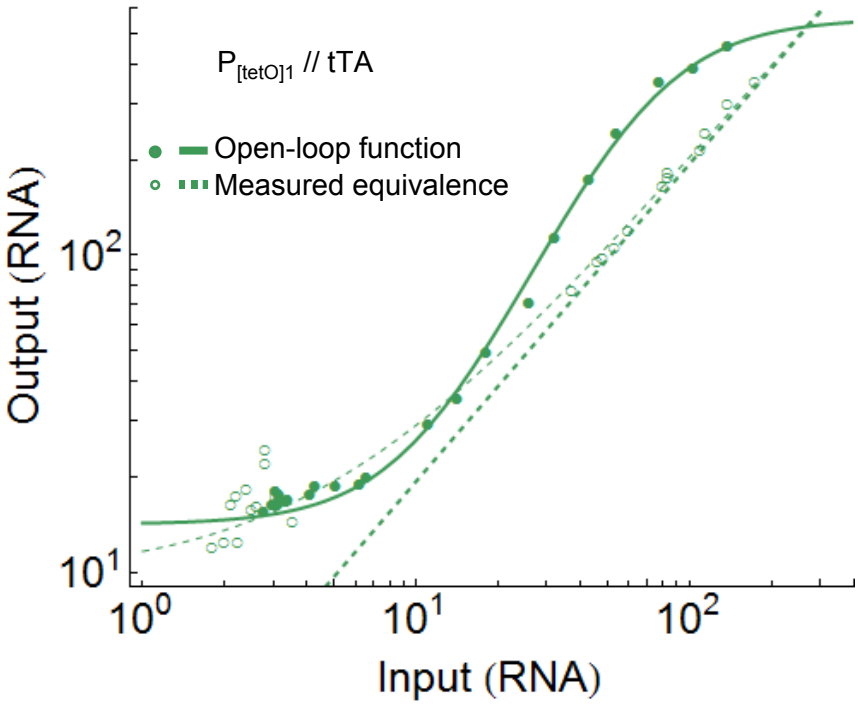

Fig. S4 Assessment of the ultrasensitivity due to the dimerization of tTA in open-loop construct. The input and output RNA was measured by varying the activity of the GAL promoter with estradiol at 0.012 μM doxycycline in $P_{[tetO]1}$-tTA Input/Output cell. The data for the open-loop function were fitted to Hill function with basal term and the measured equivalence to linear function, *s input* + *b*, where b is the basal expression of the output. The fitted values for open-loop function were: V_{max}=541.30, b=14.19, K_d=66.57, n=2.00. The thick dashed lines for the measured equivalence are the linear function without b.

Supplementary Tables

Table S1. Yeast strains.

Diploid Strain	Haploid parents	Integration locus (plasmid)			Function
	A alpha	*ade2:: **ADE2**_*	*ura3:: **URA3**_*	*his3:: **HIS3**_*	
Yvj87.2*	Yvj79.2		P_[tetO]7- *CYC1*c ǀ SL_5[AT]1 ǀ rtTA (pCH068)	P_*MRP7* ǀ GEV (pPR1)	Feedback
	Yvj70.1	P_*GAL1*UAS-*CYC1*c ǀ SL_5[AT]1 ǀrtTA (pVJ46)	P_[tetO]2- *CYC1*c ǀ *yEGFP* (pABG10)		
Yvj99*	Yvj89.1		P_[tetO]1- *CYC1*c ǀ SL_5[AT]2 ǀ rtTA (pVJ42)	P_*MRP7* ǀ GEV (pPR1)	Feedback
	Yvj91.6	P_*GAL1*UAS-*CYC1*c ǀ SL_5[AT]2 ǀrtTA (pCH094)	P_[tetO]2-*CYC1*c ǀ *yEGFP* (pABG10)		
Yvj151.3*	Yvj150.3	P_[tetO]7-TATA-[tetO]2 *CYC1*c ǀ rtTA (pMG01)		P_*MRP7* ǀ GEV (pPR1)	Feedback
	Ych178.2	P_*GAL1*UAS-*CYC1*c ǀ rtTA (pCH099)	P_[tetO]1- *CYC1*c ǀ *yEGFP* (pCH001)		
Ych260.2*	Yvj80.1		P_[tetO]7- *CYC1*c ǀ SL_5[AT]3 ǀ sc-rtTA (pCH91)	P_*MRP7* ǀ GEV (pPR1)	Feedback
	Ych250.2	P_*GAL1*UAS-*CYC1*c ǀ SL_5[AT]3 ǀ sc-rtTA(pCH102)	P_[tetO]2- *CYC1*c ǀ *yEGFP* (pABG10)		
Yvj139.1	Yvj134. 1		P_[tetO]1- *CYC1*c ǀ SL5[AT]1- ǀ tTA (pCH077)	P_*MRP7* ǀ GEV (pPR1)	Feedback
	Ych150.7	P_*GAL1*UAS-*CYC1*c ǀ SL_5[AT]1 ǀtTA (pCH085)	P_[tetO]2- *CYC1*c ǀ *yEGFP* (pABG10)		
Yvj138.48	Yvj133.4		P_[tetO]7- *CYC1*c ǀ SL_6[AT]0 ǀ tTA (pCH061)	P_*MRP7* ǀ GEV (pPR1)	Feedback
	Yvj135.8	P_GAL1UAS-CYC1c ǀ SL_6[AT]0 ǀtTA (pCH062)	P_[tetO]2- *CYC1*c ǀ *yEGFP* (pABG10)		
Yvj143	Yvj40.3			P_*MRP7* ǀ GEV (pPR1)	I/O
	Ych151.5	P_*GAL1*UAS-*CYC1*c ǀ SL_5[AT]1 ǀtTA (pCH085)	P_[tetO]1- CYC1c ǀ SL_5[AT]1 ǀ tTAΔ(45/45)::YFP (pCH066)		
Yvj142	Yvj40.3			P_*MRP7* ǀ GEV (pPR1)	I/O
	Ych107.1	P_GAL1UAS-CYC1c ǀ SL_6[AT]0 ǀtTA (pCH062)	P_[tetO]7- CYC1c ǀ SL_6[AT]0 ǀ rtTAΔ(45/45)::YFP (pCH058)		

* Constructed as described in Hsu et al (2016).